

# Urban Computing with Taxicabs

Yu Zheng<sup>1</sup>, Yanchi Liu<sup>1,2</sup>, Jing Yuan<sup>1</sup>, Xing Xie<sup>1</sup>

<sup>1</sup>Microsoft Research Asia, Beijing, China

<sup>2</sup>University of Science and Technology Beijing, Beijing, China

{yuzheng, v-jinyua, xingx,}@microsoft.com, liuyanchi@manage.ustb.edu.cn

## ABSTRACT

Urban computing for city planning is one of the most significant applications in Ubiquitous computing. In this paper we detect flawed urban planning using the GPS trajectories of taxicabs traveling in urban areas. The detected results consist of 1) pairs of regions with salient traffic problems and 2) the linking structure as well as correlation among them. These results can evaluate the effectiveness of the carried out planning, such as a newly built road and subway lines in a city, and remind city planners of a problem that has not been recognized when they conceive future plans. We conduct our method using the trajectories generated by 30,000 taxis from March to May in 2009 and 2010 in Beijing, and evaluate our results with the real urban planning of Beijing.

## Author Keywords

Urban computing, urban planning, GPS trajectory, taxicab

## ACM Classification Keywords

H.2.8 [Database Management]: Database Applications - data mining, Spatial databases and GIS;

## General Terms

Algorithms, Experimentation.

## INTRODUCTION

Ubiquitous computing has largely been applied either in relatively homogeneous rural areas, where researchers have added sensors in places such as forests and glaciers, or in small-scale, well-defined patches of the built environment, such as smart houses or rooms [7]. Attention has recently been shifting to urban areas, which are regarded as the third place between rural areas and houses, or the public place between home and work [12]. Urban areas are more complex and interesting spaces than the other two, as they are navigated both through physical movement and interpretations of social context. Though urban settings tend to be far more dynamic in terms of what and who would participate in an application or system, urban spaces also bring us a lot of opportunities in exploring novel systems

and applications facilitating people's life and serving the city. Emerging in this circumstance, urban computing comes up with the new ubiquitous computing concept where every sensor, person, vehicle, building, and street in urban areas can be used as a computing component for serving the people and the city.

Urban computing for urban planning is one of the most significant application scenarios in the urban spaces [7][12]. The advance of human civilization has given rise to the need for urban planning that integrates land use planning and transportation planning to improve the built, economic and social environments of communities. Urbanization is increasing at a faster pace than ever in many developing countries, while some modern cities in developed countries are engaging in urban reconstruction, renewal, and sub-urbanization. Therefore, we need innovative technologies that can automatically and unobtrusively sense urban dynamics and provide crucial information to urban planners.

Naturally, big cities faced with the challenges to urban planning usually have a large number of taxicabs traversing in urban areas. For example, the numbers of taxis in Mexico City, Beijing, Tokyo and Seoul are all over 60,000 respectively. Meanwhile, there are approximated 30 cities, including New York City, Shanghai, Hong Kong, London, and Paris that have more than 10,000 licensed taxis individually. To enable efficient taxi dispatch and monitoring, taxis are usually equipped with GPS sensors, which enable them to report on their location to a centralized server at regular intervals, e.g., 1~2 minutes. In other words, a lot of GPS-equipped taxis already exist in major cities around the world, generating huge volumes of trajectories everyday [5][6][15].

Essentially, GPS-equipped taxicabs can be viewed as ubiquitous mobile sensors constantly probing a city's rhythm and pulse, such as traffic flows on road surfaces and city-wide travel patterns of people. For instance, Beijing has approximately 67,000 licensed taxis generating over 1.2 million occupied trips per day (in terms of the recorded taxi trajectories). Supposing each taxi transports 1.2 passengers per trip on average, there are about 1.44 million personal trips generated by these taxis in Beijing per day. This figure is 4.2% of the total personal trips (35 million) created by all kinds of transportations including buses, subways, taxis and private vehicles within the Six Ring Road of Beijing City (reported by Beijing transportation bureau July 2010). 4.2 percent is a significant sample reflecting people's travel in

Permission to make digital or hard copies of all or part of this work for personal or classroom use is granted without fee provided that copies are not made or distributed for profit or commercial advantage and that copies bear this notice and the full citation on the first page. To copy otherwise, or republish, to post on servers or to redistribute to lists, requires prior specific permission and/or a fee.

*UbiComp '11*, September 17-21, 2011, Beijing, China.

Copyright 2011 ACM 978-1-4503-0630-0/11/09...\$10.00.

the city. Meanwhile, the traffic flow on a road can be well modeled by the mobility of taxis traveling on the road together with a large number of private vehicles and buses.

In this paper we aim to detect the flawed and less effective urban planning in a city according to the GPS trajectories of taxicabs recorded in a certain period, such as 3 months. There are two main challenges involved in this work: 1) Modeling the city-wide traffic and travel of people using taxi trajectories; 2) Embodying the flawed planning to reveal the relationship among these flaws. In our method, we first partition a city into some disjoint regions using major roads. Then, we project the taxi trajectories of each day into these regions and formulate transitions between each pair of regions. Later, we detect the salient region pairs having heavy traffic beyond the capacity of the existing connections between them. The region pairs frequently detected across many days will be regarded as the flawed planning. At the same time, we associate the individual flaws into a series of graphs reflecting the global defects of the urban planning according to the spatial and temporal properties of these flaws. The contribution of this report lies in three aspects:

- *Traffic modeling*: We model the city-wide traffic of taxis of each day using a matrix of regions. Each item in the matrix consists of a set of features representing the effectiveness of the connection between two different regions. The values of these features are derived from the taxi traces passing the two regions.
- *Flaw detection*: We seek the possibly flawed region pairs (called a skyline) from the matrix of each day using a skyline operator. We associate the skylines (of a day) into some graphs (representing global flawed planning), and mine the frequent sub-graph patterns from the graphs across a certain number of days. The mined results consist of both flawed planning and the relationship between them.
- *Real evaluation*: We evaluate our method using a series of large-scale real GPS trajectories generated by 30,000 taxis in Beijing from March to May in 2009 and 2010. As a result, we find strong data from the real urban planning of Beijing, justifying the effectiveness of our method.

The rest of the paper is organized as follows. Section 2 overviews the problem and our solution. Section 3 presents the process for modeling city-wide traffic. Section 4 describes the detection of the flawed planning. In Section 5 we evaluate our work. After summarizing the related work in Section 6, we draw our conclusions in Section 7.

## OVERVIEW

**Definition 1 (Taxi Trajectory)**: A taxi trajectory  $Tr$  is a sequence of time-ordered GPS points,  $Tr: p_1 \rightarrow p_2 \rightarrow \dots \rightarrow p_n$ , where each point consists of a geospatial coordinate set, a timestamp, and a state of occupation (with passengers or not), e. g.,  $p = (lat, long, t, o)$ .

**Definition 2. (Region)**: The map of a city is partitioned into

disjoint regions ( $r$ ) bounded by high level (i.e. major) roads. Each region may consist of a number of road segments and lands. Refer to Figure 2 for an example.

**Definition 3. (Transition)**: Given a trajectory  $Tr: p_1 \rightarrow p_2 \rightarrow \dots \rightarrow p_n$ , a directional transition  $s: r_1 \rightarrow r_2$  is generated between  $r_1$  and  $r_2$  if  $p_i$  is the first point (from  $Tr$ ) falling in region  $r_1$  and  $p_j$  is the first point (from  $Tr$ ) falling in region  $r_2$  ( $i < j$ ). A transition  $s$  is associated with a leaving time ( $p_i, t$ ), an arriving time ( $p_j, t$ ), and a travel distance  $d$  and speed  $v$  calculated according to Equation 1 and 2.

$$d(p_i, p_j) = \sum_{i \leq k < j} Dist(p_k, p_{k+1}), \quad (1)$$

$$v = d(p_i, p_j) / |p_j.t - p_i.t|, \quad (2)$$

$Dist(p_k, p_{k+1})$  denotes the Euclidian distance between two consecutive GPS points.

Figure 1 presents the architecture of our method, which consists of two major components: 1) modeling city-wide traffic based on taxi trajectories and 2) detecting flawed planning. We will detail each step of these two components in the following two sections respectively.

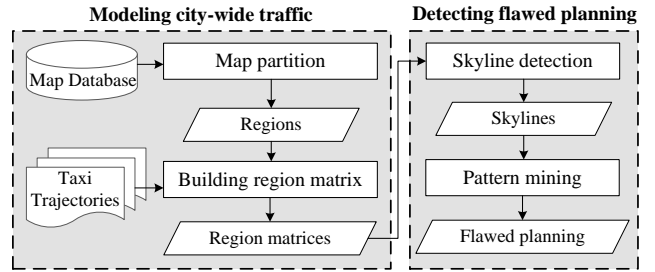


Figure 1. The architecture of our method

## MODELING CITY-WIDE TRAFFIC

This component first partitions a map of a city into some regions, and then builds a set of region matrices that correspond to different time of day and day of week.

### Map Partition

As shown in Figure 2, we partition the urban area of Beijing into disjoint regions using major roads (like the red and blue roads). Each region stands for a community including some neighborhoods and low-level road segments (denoted as gray polylines). The partition method carries more semantic meanings of people’s travel than using a uniform grid-based partition. At the same time, we conduct our research based on regions instead of road segments for two reasons. First, traffic problems appearing on roads are just observations, while regions carrying rich knowledge about people’s living and travel are the source of the problem. Second, flaws represented by regions contribute to both land use and transportation planning. However, the road segments can only help transportation planning. For instance, if the connection between two regions are determined to be less-effective, the possible solution for fixing this flaw could be building new roads between them (pertaining to transportation planning), or adding some local businesses, e.g., shopping malls, in the region outsourcing people (i.e., land use planning).

Here, we employ Connected Components Labeling (an image segment method) [11] to segment a map into regions effectively and efficiently, as the problem of subdivisions in a polygonal region is NP-complete.

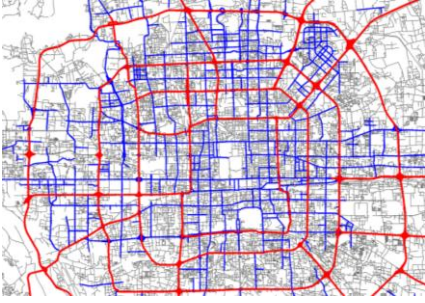


Figure 2. Heat map of the partitioned regions in Beijing

### Building Region Matrix

This process is comprised of the following three steps.

1) *Temporal partition*: In this step, we first partition the taxi trajectories into two parts according to workday and rest day (consisting of weekends and public holidays) since people’s travel on these two types of days are different. Then, we further segment time of day into some slots in terms of the traffic conditions in the city.

First, in the same time slot, the traffic conditions and the semantic meaning of people’s travel are similar. For example, Figure 3 A) shows the average travel speed of all the taxis (with passengers) in Beijing at different times of workdays. The average travel speed of the entire city of Beijing as defined previously in time slot 7:00-10:30am is lower than that of the entire day. This matches the generally accepted assumption that people are going to work during the morning rush hours. Likewise, the time slot of 4pm-7:30pm corresponds to the evening rushing hour in the workday when people go home. Second, if we do not respectively explore the trajectories from different time slots, we will miss some actually flawed planning as the detected results could be dominated by some regions only having heavy traffic in a particular time slot. Third, the time partition enables us to explore the temporal relations between the results detected from continuous time slots, helping us deeply understand the flaws. We will further justify the temporal partition later.

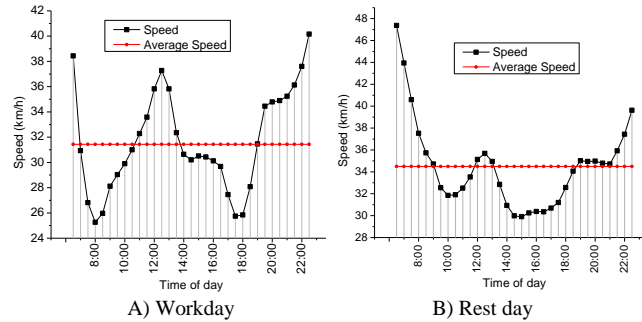


Figure 3. Traffic conditions in Beijing changing over time

According to Figure 3, we obtain the time slots shown in Table 1. Later, we build a region matrix for each time slot of each day (refer to the following paragraphs).

Time	Work day	Rest day
Slot 1	7:00am-10:30am	9:00am-12:30pm
Slot 2	10:30am-4:00pm	12:30pm-7:30pm
Slot 3	4:00pm-7:30pm	7:30pm-9:00am
Slot 4	7:30pm-7:00am	

Table 1. Time partition for workdays and rest days

2) *Transition construction*: We pick out the effective trips with passengers from taxi trajectories in terms of the occupancy state associated with a sample (a weight sensor is embedded in a taxi to detect whether there are additional persons beside a driver in the taxi). So, an effective taxi trajectory represents a passenger’s trip. Then, we project these trajectories onto the map and construct transitions between two regions according to definition 3. As demonstrated in Figure 4, two trajectories,  $Tr_1$  and  $Tr_2$ , respectively traversing  $r_1 \rightarrow r_3$  and  $r_1 \rightarrow r_2 \rightarrow r_3$ , formulate four transitions:  $r_1 \rightarrow r_3$ ,  $r_1 \rightarrow r_2$ ,  $r_2 \rightarrow r_3$ , and  $r_1 \rightarrow r_3$ , denoted as the blue arrows. Note that, a trajectory discontinuously traversing two regions, such as  $r_1 \rightarrow r_3$  in  $Tr_2$ , still formulate a transition between the two regions. The distance  $d$  of this transition is  $\sum_{4 \leq k < 8} Dist(p_k, p_{k+1})$ , and the travel speed is approximately  $d/(p_8.t - p_4.t)$ .

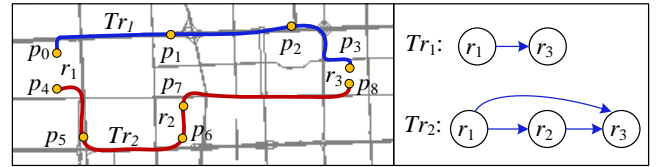


Figure 4. Transfer a trajectory into transitions

**Definition 4 (Region Pair)**. A region pair is a pair of regions ( $r_1 \rightarrow r_2$ ) having a set of transitions (between them). By aggregating the transitions, each region pair is associated with the following three features: 1) volume of traffic between these two regions, i.e., the count of transitions  $|\mathcal{S}|$ , and 2) expectation of these transitions’ speeds  $E(V)$ , and 3) ratio  $\theta$  between the expectation of the actual travel distance  $E(D)$  and the Euclidian distance between the centroids of two regions,  $CenDist(r_1, r_2)$ .

$$E(V) = \frac{\sum_{s_i \in \mathcal{S}} s_i.v}{|\mathcal{S}|}, \quad (3)$$

$$E(D) = \frac{\sum_{s_j \in \mathcal{S}} s_j.d}{|\mathcal{S}|}, \quad (4)$$

$$\theta = E(D)/CenDist(r_1, r_2), \quad (5)$$

Where  $\mathcal{S}$  is the collection of transitions between  $r_1$  and  $r_2$ .

Figure 5 plots the region pairs from a time slot 7-10:30am in a workday in the  $\langle |\mathcal{S}|, E(V), \theta \rangle$  space. A black point represents a region pair. The projections of these region pairs on XZ and YZ spaces are also visualized with green and blue plots. Note that the value of a given  $\theta$  could be smaller than 1 as taxis might cross two adjacent regions with a distance shorter than that between the two centroids.

Some might be concerned with the transitions generated by the trajectories discontinuously passing two regions, e.g.,

$Tr_2$  traveling from  $r_1$  to  $r_3$  in Figure 4, in which a taxi visited several other regions before reaching  $r_3$ . We can analyze this problem from two perspectives. First, the connectivity of the two regions should be represented by all the possible routes between them instead of the fast (or direct) transitions. Sometimes, reaching a region through a roundabout route passing other regions is also a good choice to avoid traffic jams. Second, these discontinuous transitions do not bias the  $E(V)$  and  $\theta$ . If there is an effective shortcut between two regions (e.g.,  $Tr_1$ ), most taxis intending to travel from  $r_1$  to  $r_3$  will still take the shortcut instead of the roundabout route. That is, the amount of discontinuous travel is only a small portion in the transition set. As a result,  $E(V)$  and  $\theta$  are still close to the real travel speed and ratio that people could travel from  $r_1$  to  $r_3$ . On the contrary, if all the taxis have to reach  $r_3$  by passing additional regions, e.g.,  $r_2$ , that means the route directly connecting  $r_1$  and  $r_3$  is not very effective.

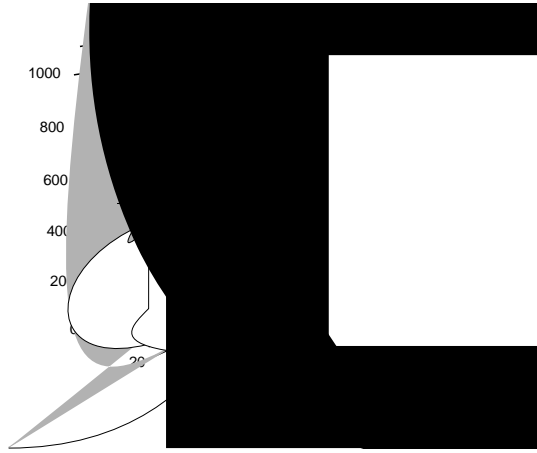


Figure 5. Distribution of region pairs in the workday

3) *Build region matrix*: We formulate a matrix of regions  $M$ , as demonstrated in Figure 6, for each time slot in each day. An item in the matrix is a tuple,  $a_{i,j} = \langle |\mathcal{S}|, E(V), \theta \rangle$ , denoting the number of transitions, expectation of travel speed, and  $\theta$  between region  $r_i$  and  $r_j$ . Supposing there are  $x$  workdays and  $y$  rest days,  $4x + 3y$  matrices will be built if using the scheme of the time slots shown in Table 1.

$$M = \begin{matrix} & r_0 & r_1 & \dots & r_j & \dots & r_{n-1} & r_n \\ r_0 & \phi & a_{0,1} & \dots & \dots & \dots & \dots & a_{0,n} \\ r_1 & a_{1,0} & \phi & \dots & \dots & \dots & \dots & a_{1,n} \\ \vdots & \dots & \dots & \dots & \dots & \dots & \dots & \dots \\ r_i & a_{i,0} & a_{i,1} & \dots & a_{i,j} & \dots & \dots & a_{i,n} \\ \vdots & \dots & \dots & \dots & \dots & \dots & \dots & \dots \\ r_{n-1} & a_{n-1,0} & \dots & \dots & \dots & \dots & \phi & a_{n-1,n} \\ r_n & a_{n,0} & \dots & \dots & \dots & \dots & \dots & \phi \end{matrix}$$

Figure 6. Region matrix and the properties of each item

### DETECTING FLAWED URBAN PLANNING

We first detect the skyline of each region matrix in terms of the values of each tuple. Then, we mine graph patterns representing flawed planning from these skylines.

### Skyline Detection

$\langle |\mathcal{S}|, E(V), \theta \rangle$  will model the connectivity and the traffic between two regions. Specifically,  $\theta$  captures the geometric property of the connection between a pair of regions. A region pair with a big  $\theta$  means people have to take a long detour traveling from one region to the other.  $E(V)$  and  $|\mathcal{S}|$  represent the features of traffic. A big  $|\mathcal{S}|$  and small  $E(V)$  imply heavy traffic carried by the existing routes between two regions. In this step, we aim to retrieve the region pairs with a big  $\theta$ , small  $E(V)$  and large  $|\mathcal{S}|$ , which indicate flawed urban planning.

We first select the region pairs having the number of transitions above the average from a matrix  $M$ . Then, we find the skyline set  $L$  from these selected region pairs according to  $E(V)$  and  $\theta$ , using skyline operator [1].

**Definition 5. (Skyline)**: The skyline is defined as those points which are not dominated by any other point. A point dominates another point if it is as good or better in all dimensions and better in at least one dimension.

Specifically, in our application, each  $a_{i,j} \in L$  is not dominated by others,  $a_{p,q} \notin L \wedge a_{p,q} \in M$ , in terms of  $E(V)$  and  $\theta$ . That is, there is no region pair  $a_{p,q} \notin L$  having a lower speed and bigger  $\theta$  than  $a_{i,j} \in L$ . Figure 7 A) depicts an example of the skyline set  $L$  using a blue dash line where a point denotes a region pair. Clearly, no blank points simultaneously have a smaller  $E(V)$  and bigger  $\theta$  than the points from the  $L$ .

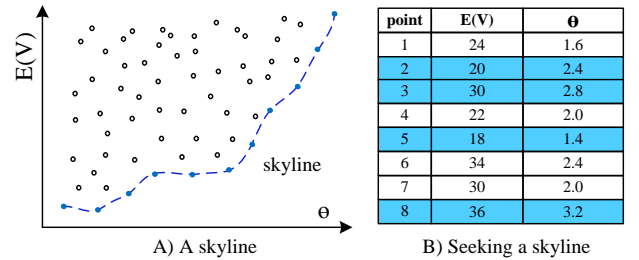


Figure 7. An example of skyline detection

Figure 7 B) shows the process for seeking the skyline. For example, point 1 does not pertain to the skyline because it is dominated by point 2. However, point 2 does not dominate point 3 as point 3 has a bigger  $\theta$  than point 2. Likewise, point 5 and 8 are detected as the skyline while point 4, 6, and 7 are dominated by the skyline.

The detected skyline is comprised of three kinds of region pairs. 1) A region pair with a very small  $E(V)$  and  $\theta$ , illustrated in Figure 8 A). This means two regions are connected with some direct routes while the capacity of these routes are not sufficient as compared to the existing traffic between the two regions. The small  $E(V)$  and  $\theta$  also indicate that people have no other choice (even if it is a detour) but to take these ineffective routes for traveling between the two regions. Otherwise, the  $\theta$  will become bigger. 2) A region pair with a small  $E(V)$  and big  $\theta$ , shown in Figure 8 B). This denotes that people have to take detours for travelling between two regions while these

detours suffer from heavy traffic leading to a slow speed. This is the worst case among these three situations. 3) A region pair with a big  $E(V)$  and big  $\theta$ , depicted in Figure 8 C). These two values imply that people travel between two regions by taking some far detours which are fast, e.g., a high way. Though the speed is not slow, the long distance will cost people a lot of time and gas. So, the connectivity between such kinds of regions still has flaws.

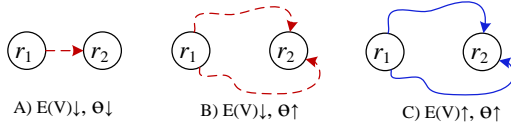


Figure 8. Three kinds of region pairs in a skyline

Note that we focus on finding the most salient flawed urban planning instead of all the poor ones. Seeking the skyline from the region pairs with a large volume of traffic ( $|\mathcal{S}|$  is above the average), we guarantee 1) the detected skyline is related to many people's travel and 2) each  $(E(V), \theta)$  is calculated based on a large number of observations.

### Pattern Mining from Skylines

In this step, we first build a skyline graph for each day by connecting the region pairs in the skylines of different time slots. Then, we detect the sub-graph patterns from these graphs using a graph pattern mining algorithm [13].

1) *Formulating skyline graphs*: As demonstrated in Figure 9, there is a skyline in each time slot (denoted as a row) of each day (represented by a column). Two region pairs from two consecutive slots are connected if they are spatially close to each other. For example, in Day 1 we connect the region pair  $(r_1 \rightarrow r_2)$  from slot 1 to  $(r_2 \rightarrow r_8)$  from slot 2, because these two region pairs share the same node  $r_2$  and appear in the consecutive time slots of the same day. Likewise,  $(r_4 \rightarrow r_5)$  to  $(r_5 \rightarrow r_7)$  from these two slots are connected. However,  $(r_4 \rightarrow r_5)$  from slot 1 and  $(r_8 \rightarrow r_4)$  from slot 3 cannot be connected as they are not temporally close. The built skyline graphs are shown in the fourth column. Note that, there could be multiple isolated graphs pertaining to a day like day 2.

2) *Mining frequent sub-graph patterns*: We mine the frequent sub-graph patterns from the skyline graphs  $\mathbb{G}$  across a certain number of days for two reasons. One is to avoid any false alteration. Sometimes, a region pair with effective connectivity could be detected as a part of skyline because of some anomaly events, such as traffic accidents. The other is to provide a deeper understanding of the flawed planning. By associating individual region pairs, we can find the causality and relation among these regions, which is more valuable for understanding how a problem is derived. The bottom of Figure 9 shows the mined skyline patterns using different supports. Here, the support of a sub-graph pattern  $g$  is calculated as Equation 6, where  $G$  is a skyline graph containing the sub-graph  $g$  and  $\mathbb{G}$  is the collection of skyline graphs across days. The denominator denotes the number of days that the dataset across.

$$Support(g) = \frac{|\{G|g \subseteq G, G \in \mathbb{G}\}|}{num\ of\ days}, \quad (6)$$

For instance, the support of  $(r_4 \rightarrow r_5)$  is 1 since it appears in the skyline graphs of all three days while that of  $(r_3 \rightarrow r_6)$  is  $2/3$  as it only appears in Day 2 and Day 3. Given a threshold  $\delta$  we can choose the patterns with the support  $\geq \delta$ . These patterns represent the flawed urban planning which is salient and appears frequently.

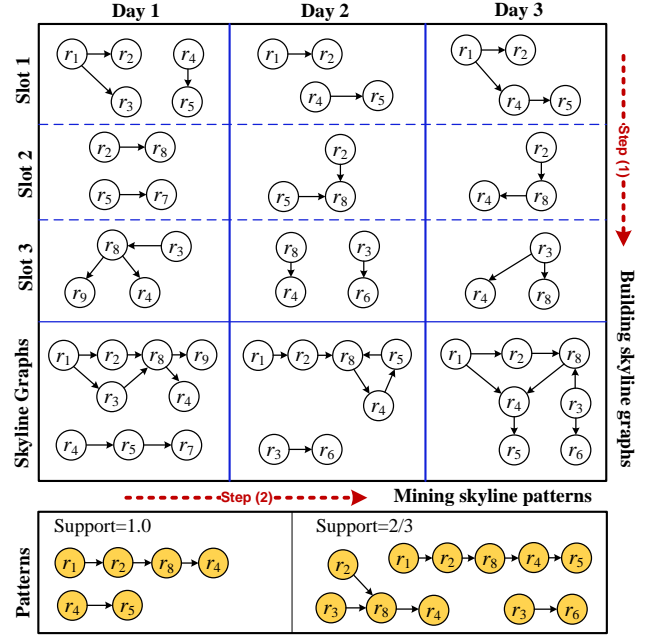


Figure 9. Mining frequent skyline patterns

Besides, we mine the association rules among these patterns according to Equation 7 and 8 where  $|g_1 \cup g_2|$  denotes the number of days that  $g_1$  and  $g_2$  co-occurred and  $|g_1|$  means the number of days having  $g_1$ . Two patterns formulate an association rule, denoted as  $g_1 \Rightarrow g_2$ , if the support of  $g_1 \Rightarrow g_2 \geq \delta$  and its confidence  $\geq \theta$  (a given threshold).

$$Support(g_1 \Rightarrow g_2) = \frac{|g_1 \cup g_2|}{num\ of\ days}, \quad (7)$$

$$Confidence(g_1 \Rightarrow g_2) = \frac{|g_1 \cup g_2|}{|g_1|}. \quad (8)$$

For example, as depicted in Figure 9,  $(r_4 \rightarrow r_5) \Rightarrow (r_3 \rightarrow r_6)$  whose support is  $2/3$  and confidence is  $2/3$ , while the confidence of  $(r_3 \rightarrow r_6) \Rightarrow (r_4 \rightarrow r_5)$  is 1.

The mined association rules can consist of over 2 patterns. For instance,  $g_1, g_2 \Rightarrow g_3$ , i. e.,  $g_3$  has a very high probability (conditioned by  $\delta$  and  $\theta$ ) to occur when  $g_1$  and  $g_2$  appear simultaneously. Meanwhile, these association rules may not be geospatially close to each other, hence revealing the causality and correlation between the flawed planning that seems to have no relationship in the geospaces. The experiments include more examples.

## EVALUATION

### Settings

In this section, we carry out our method with a large-scale taxi trajectory dataset generated in Beijing in the past two years, and evaluate the detected results based on the real urban planning published by the government of Beijing.

**Taxi trajectories:** Table 2 shows the properties of the two trajectory datasets that we used for evaluating our method. We select the data from the same time span within a year in case people have different travel patterns in different seasons. The latter is slightly larger and denser as some expired taxis are replaced by new taxis with better facilities.

Datasets		2009.3-5	2010.3-6
Number of taxis		29,286	30,121
Effective days		89	116
Number of points	Total	679M	1,730M
	Per taxi/day	306	528
Distance (KM)	Total	310M	600M
	Per taxi/day	128	171
Average sampling rate (s)		100	74
Ave. dist. between two points (m)		457	349

**Table 2. Two datasets of taxi trajectories used for evaluation**

**Map data:** We use the road network data of Beijing, which has 106,579 road vertices and 141,380 road segments. We pick out 25,262 major road segments with level 0, 1, and 2 (0 is the highest level representing highways, 6 is the lowest denoting small streets) to partition the urban area of Beijing into some regions. As a result, we obtain 444 regions.

We verify the detected flaws in the following two ways:

- 1) We select some urban planning, such as new subway lines and roads, which has been implemented for use between the times of the two datasets, and study whether the carried out planning reduces the flaws existing in the former dataset.
- 2) We check if some flaws that have been detected in both two datasets by our method embodied in the future urban planning of Beijing (i. e., the problem of these regions has been recognized by the city planner).

We compare our approach with a baseline method which retrieves the top hottest regions in Beijing according to the following metric  $q$ , where  $l$  denotes the road segments falling in the region  $r$ .

$$q = \frac{\text{number of taxis ending at } r}{|\text{time}| \sum_{l \in r} l.\text{length}}, \quad (9)$$

This metric represents the density of taxis sending people to a region in a unit time slot (hour). Here, the total length of road (in a region) makes more sense beyond the area size of the region since the length (and capacity) of roads reflect the real spaces that vehicles can travel. Meanwhile, we do not differentiate the capacities of the road segments in a region any longer as all of them are local streets. We will show the heat maps of Beijing in terms of this metric later.

## Results

Figure 10 and 11 present the distributions and trends of  $\langle |\mathcal{S}|, E(V), \theta \rangle$  changing over time of day in the urban area of Beijing on workdays and rest days respectively. The value shown in each figure is an average result across a number of days (from the dataset of 2010). The trends and distributions of 2009 are similar to those of 2010, though the exact values have minor differences. So, we do not show them in our paper. The two sets of figures present two

aspects of information. First, they demonstrate the clear differences (of distributions and trends) between workdays and rest days and among different time slots, justifying the importance of temporal partition. Second, the three features (we used to detect flawed planning) well reflect on people’s mobility patterns and traffic at a city-wide level. A lot of commonsense knowledge and interesting stories can be found in these figures, validating their effectiveness.

For example, as illustrated in Figure 10 A) and Figure 11 A), the morning rush hour on the rest days comes 2 hours later than workdays, which denotes that on average people start outdoor activities on the rest days (in Beijing) 2 hours later than on the workdays. However, the rest days and work days have the same evening rush hours at 6pm. This denotes people always keep their time for dinner which is important to them no matter the day of the week and when they get up. Meanwhile, workdays have a slightly heavy traffic in the morning rush hours than in the evening one; on the contrary, the rest days have an opposite result. Figure 10 C) contains two clear peaks (at 10am and 5pm) where the number of region pairs with a  $\theta$  greater than 1.2 increases rapidly, while those where  $\theta < 1$  remain stable. This denotes that more taxi drivers have to take a slight detour to reach a destination quickly during rush hours instead of choosing the shortest path as they can at other times (since the direct paths become crowded). That could mean the taxi fare increases during rush hours.

			2009	2010
Workdays	Average # of region pairs in a skyline	Time slot 1	7.65	9.09
		Time slot2	7.40	7.05
		Time slot 3	7.35	7.29
		Time slot4	6.70	7.82
	Skyline graphs	# of nodes	12.93	16.18
		# of links	8.40	10.81
Rest days	Average # of region pairs in a skyline	Time slot 1	6.68	7.97
		Time slot2	6.68	7.66
		Time slot 3	6.66	7.37
	Skyline graphs	# of nodes	11.91	14.49
		# of links	7.05	8.86

**Table 3. Properties of the detected skylines and skyline graphs**

Table 3 shows the properties of the skylines detected from each time slot and the graph formulated for a day. The values are averages across a number of days. First, the size of the skylines and graphs becomes slightly larger in 2010 as compared to 2009. For instance, the skyline of time slot 1 (7am-10:30am) in a workday contains on average 7.65 region pairs in 2009 while this number reaches 9.09 in 2010. At the same time, the number of nodes, i.e., regions (refer to Figure 9 for an example) in a skyline graph also increased from 12.93 (in 2009) to 16.18 (in 2010) in the workdays. These results indicate that the traffic conditions in Beijing become worse in 2010 than 2009 (the figures of these two years are comparable since the number of taxis in these two years are similar and we have divided the counts by days, i.e., irrelevant to the period of time). Second, the skylines of workday have a bigger number of region pairs

than the rest days, leading to a larger size of skyline graph in workday as well. This trend occurs in both years, denoting that people's mobility is relatively more focused

on rest days (shopping and entertainment areas are more likely to be the destinations) while they would travel to a variety of locations on workdays for more purposes.

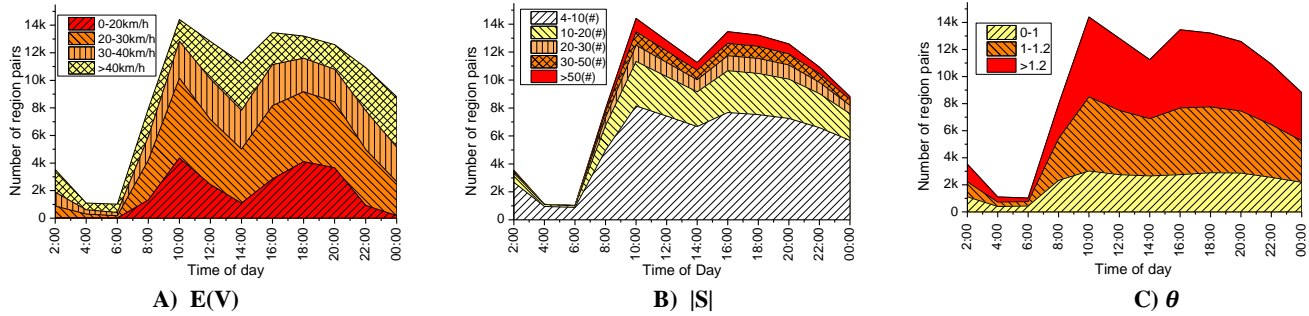


**Figure 10. Distribution and trend of workday changing over time of day (in urban areas of Beijing):** In these figures Y axis is the number of region pairs. For instance, as shown in Figure 10 A), at 10am on work days, there are about 4,000 (4k) region pairs whose  $E(v) \leq 20\text{km/h}$  and 6k regions pairs with a  $20\text{km/h} < E(V) \leq 30\text{km/h}$ .

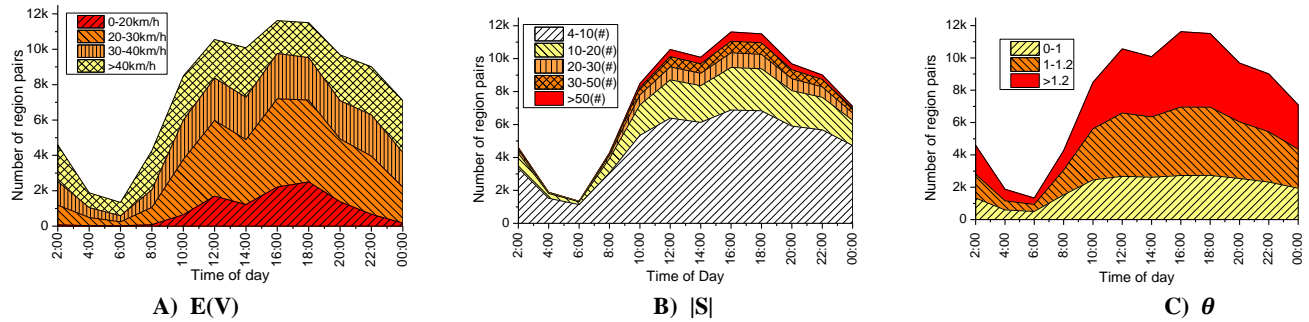


**Figure 11. Distribution and trend of the rest days changing over time of day (in urban areas of Beijing):** In these figures Y axis is the number of region pairs. For instance, as demonstrated in Figure 11 B), at 6pm on rest days, there are approximately 6k region pairs whose  $4 \leq |S| < 10$  and 3k region pairs having  $10 \leq |S| < 20$ .

Table 4 presents the number of trips (with passengers) that a taxi generated in different time slots in 2009 and 2010 respectively. Clearly, the numbers of 2010 become smaller than those of 2009, which means taxi drivers took fewer passengers than before. The major reason causing this is that the average travel speed of a taxi sending a passenger to a destination becomes lower, increasing the travel time of a single trip (as shown in the two bottom rows of Table 4). In short, the traffic conditions of Beijing become worse in 2010 (compared with 2009). It is not difficult to understand this result given that the number of auto mobiles in Beijing has reached 4.8 million with a rapid growth of 800,000 from 2009 to 2010, reported by Beijing Traffic Management Bureau. At the same time, the number of residents in Beijing exceeded 19 million in 2010 with a growth of over 560,000 from 2009. Moreover, as Beijing has been becoming an advanced city, a significant number of flowing population (e.g., 184 million tourists, i.e., over 0.5 million per day) have traveled to Beijing in 2010, generating addition traffic. The other reason is that some newly built transportation systems, such as subway lines, change the transportation modes of some people who took taxis previously in some regions. Also, a few people traveling by taxis before bought their own private cars in 2010. But, the number of people expecting to take a taxi may not decrease in Beijing as the added population could be larger than the number reduced by the second reason.

	Slots	Workday			Rest days			
		1	2	3	1	2	3	
Trip	2009	3.1	4.6	3.2	3.8	2.0	5.0	4.3
	2010	2.7	4.4	2.9	3.7	1.7	4.5	3.9
Speed km/h	2009	29.6	34.2	29.1	42.3	33.4	32.8	41.7
	2010	28.0	32.7	28.3	40.8	32.9	32.0	41.0

**Table 4. Number of trips per taxi per day and average speed:** The actual number of trips could be slightly bigger as we remove some trips with sensor signal error. Both years have a similar portion of such data, hence the gap is correct.

The indication derived from Table 3 and 4 is also embodied by the heat maps of Beijing shown in Figure 12, where the color of most regions becomes shallower in 2010 than 2009, especially in some hot areas. This denotes that the number of passengers that reach a region in a unit time decreased. Actually, the transportation and land use of these hot regions do not change while the population of Beijing increased in 2010. In short, the number of people expecting to take a taxi should increase in these areas. The only reason leading to this result is that the travel speed of taxis in these regions decreased. However, a few regions, like Wangjing area located in the East-West corner of the 4<sup>th</sup> Ring Road, have attracted more people with its recent development (many companies, shopping malls and restaurants have been built here), becoming deeper in color.

However, the hot regions may not be the defects in urban planning though very likely to be, while some regions

which are not that hot could have flaws. Additionally, the heat map does not reveal the relation between the flawed regions. To address these issues, Figure 13 presents the flawed urban planning (frequent sub-graph patterns) determined by our method in 2009 and 2010 respectively.

Clearly, there are some regions, which are not very hot, that have been detected as flawed planning (we will evaluate these regions later). By comparing these two sets of figures, we observe the following two aspects:

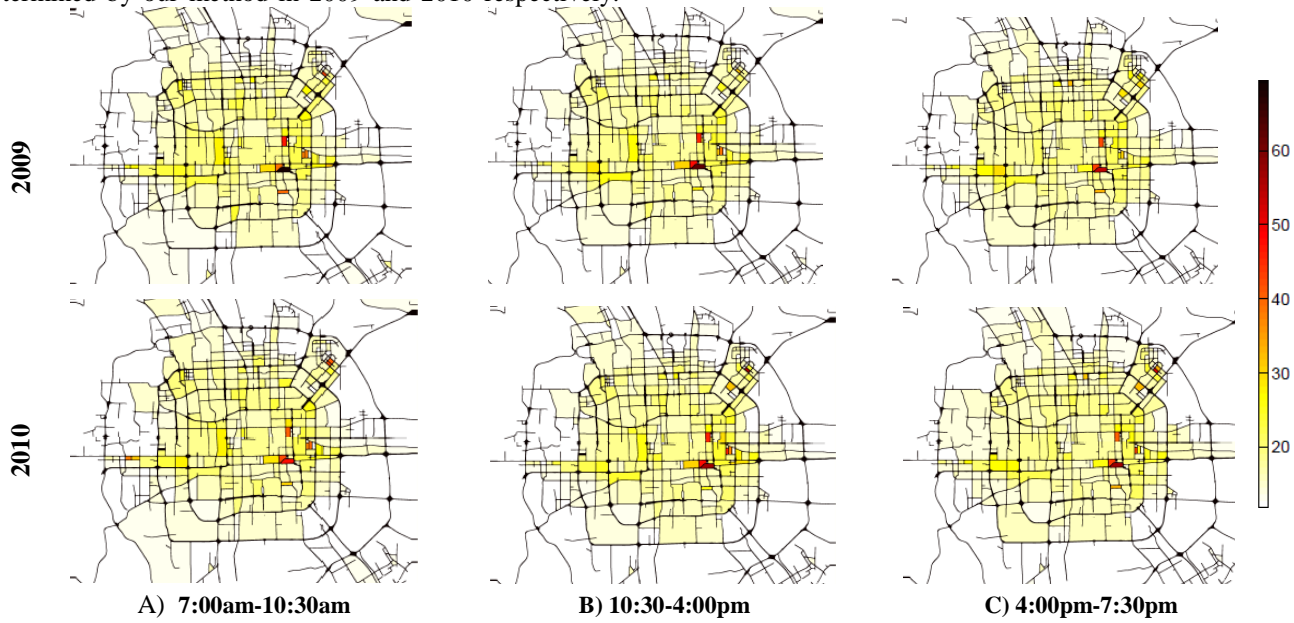


**Figure 12.** Heat maps of Beijing of the same workday from different two years 2009/5/12 and 2010/5/12 according the  $q$ : The depth of color filling a region stands for the number of people reaching a region by taxis in an hour (refer to Equation 9 for details).



**Figure 13.** The flawed urban planning detected based on the taxi trajectories of 2009 and 2010 in the workdays and rest days: The color of a region denotes the frequency that a region has been detected as a flaw (the deeper means more frequent), and the arrows represent the direction of transition between two regions. The first row shows the results of 2009 and the second row stands for 2010. Figures in the left column pertain to workdays and the other column belongs to the rest days. The results are frequent sub-graph patterns with a support  $\geq 0.06$ . Clearly, a hot region shown in Figure 12 might not be the region with frequent traffic problem, vice versa.



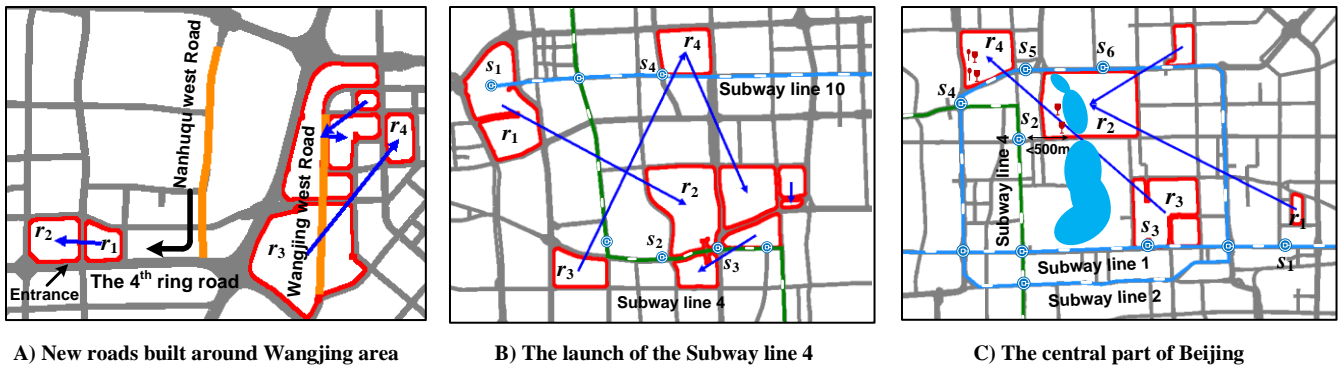


Figure 14 Illustration on the flawed planning that appeared in 2009 while disappearing in 2010

1) *Some flawed planning occurring in 2009 disappeared in 2010.* As shown in Figure 14 A), some region graphs like  $(r_1 \rightarrow r_2)$  disappeared in 2010 because of the two newly built roads (depicted as the yellow lines). These two roads were opened between the times of the two datasets. Before the launch of Nanhuqu west road in August 2009, people living in the areas above the 4<sup>th</sup> ring road in this figure had to enter the 4<sup>th</sup> Ring Road (a high way) using the only entrance located in  $r_2$ . Now, a significant portion of people can reach the 4<sup>th</sup> Ring Road by taking the Nanhuqu west road directly; hence not necessarily travel to  $r_2$  by passing  $r_1$ . Similarly, regions like  $(r_3 \rightarrow r_4)$  disappeared in Wangjing area with the launch of the Wangjing west road, as people have additional ways for traveling among them.

Other examples demonstrated in Figure 14 B) and C) reveal the effect of subway line 4 (launched in September 2009) on urban planning in Beijing. Before the launch,  $(r_1 \rightarrow r_2)$  shown in Figure 14 B) had traffic problems according to the results of our method. However, with the subway line 4 more people can reach  $r_2$  by taking subway systems with a one-stop transfer (e.g., starting at subway station  $s_1$  in line 10 and ending at  $s_2$  or  $s_3$  in line 4). This transport mode is faster and cheaper than by a taxi. Similar explanations can also be applied to other flawed urban planning having disappeared in Figure 14 B). Figure 14 C) illustrates two interesting stories, reflecting on how the subway line 4 affects the traffic of the central part of Beijing, where  $r_1$  belongs to central business district and regions within the subway line 2 contains a lot of famous tourist attractions, such as Houhai bar street along Houhai lake in  $r_2$  and Wangfujing pedestrian street in  $r_3$ . Previous, many people went to Houhai bar street from  $r_1$  by taxis after finishing their business. Though there is a subway station  $s_6$  on line 2 close to  $r_2$ , most bars are located in the west side of the lake, leading to a 20-minute walk distance to a traveler. After the launch of the subway line 4, there is a subway station  $s_2$  with a distance smaller than 500 meters to the bar street. Consequently, people have additional choices for their trips. A similar story can be found in the disappeared flaw  $(r_3 \rightarrow r_4)$ , where people travel to  $r_4$  for diner after visiting  $r_3$  while most restaurants are located close to  $s_4$ .

2) *The number of regions having defects increased in 2010 beyond 2009 and some flaws occurring in 2009 still exist.*

Figure 15 demonstrates some flawed planning (represented by frequent sub-graph patterns) that still exists in 2010. The blue polyline shown in Figure 15 A) is the subway line 15 (which was partially launched in Dec. 2010 after the time of the trajectory data), and the green one stands for line 14 (which is still under construction). The planning of these two subway lines denotes that the urban planner has recognized the problem existing in the regions, justifying the validity of the results generated using our method. Furthermore, we specify the linking structure between these regions. For example, region  $r_1$ ,  $r_2$  and  $r_3$  formulate a graph pattern, which means that they often appear together. Such kind of graph patterns reveals the relation between individual flawed regions and presents a comprehensive view on the defects of a plan. So, when designing a new plan, a city planner cannot only discover regions with problems but also understand the flaws systematically.

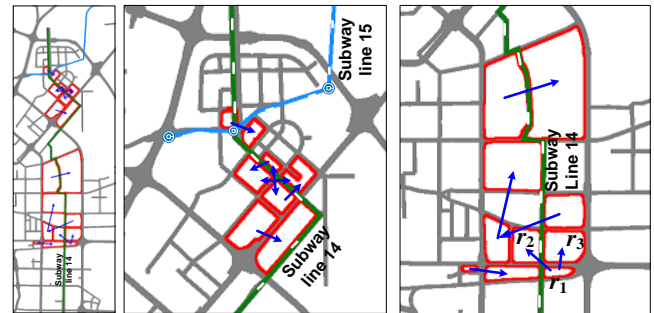


Figure 15. Subway Lines 14 and 15 and related existing flaws

From the result presented in Figure 13, we also find some association rules between the detected graph patterns. Figure 16 illustrates an example,  $(r_1 \rightarrow r_2) \Rightarrow [(r_2 \rightarrow r_4), (r_1 \rightarrow r_3)]$  with support=0.05 and confidence=0.7. In short,  $(r_2 \rightarrow r_4)$  and  $(r_1 \rightarrow r_3)$  have a probability of 0.7 to appear if  $(r_1 \rightarrow r_2)$  occurs. This pattern suggests that many people leaving  $r_1$  are heading to regions  $r_3$  and  $r_4$  while  $r_2$  becomes the bottle-neck of these transitions. Such kind of implied problem is not easy to find (without using our method), as sometimes the detected regions may not be geospatially close. For instance,  $r_3$  is not close to  $r_2$ , and  $r_4$  is not adjacent to  $r_1$ . Due to the limited spaces, we will show more interesting results and a live demo during the presentation at the conference.

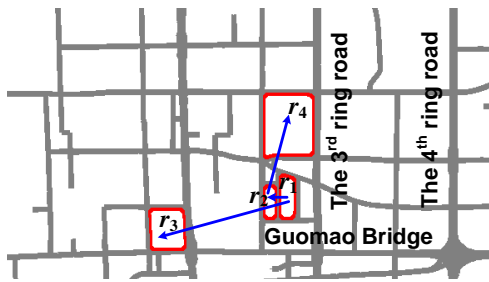


Figure 16. Association rules mined from the data of 2010

## RELATED WORK

### Mining Taxi Trajectories

A significant number of published documents have presented work aiming to mine the trajectories of taxicabs since the trajectory data has recently become widely available. They [5][10] studied taxi drivers' pick-up behavior in creating higher profit (e.g., how to easily find passengers) by analyzing fleet trajectories. Paper [16] presents some probabilistic models predicting a driver's destination and route based on historical GPS trajectories. Paper [6] estimates the real-time traffic flows on some road segments in terms of the recently received taxi trajectories. Yuan et al. [14][15] learn the practical, driving path to a destination from taxi trajectories, considering that taxi drivers are experienced drivers. Different from the above-mentioned work, we mine taxi trajectories for supporting urban planning instead of for an end user. We are the first team to carry out such studies for this purpose.

### Urban Computing

The advances of ubiquitous computing technology have brought considerable attention to urban computing in recent years [7][12]. Most literature discusses the urban computing from the perspective of social computing in the urban area, e.g., estimating the similarity between users in terms of their location histories [2][3][9], extracting social structures from mobile phone data [4], enabling friend and location recommenders in the real world [17][18], and studying the influence of pervasive systems on people in urban spaces [8]. Different from these studies, we explore the urban computing from the perspective of urban planning, sensing people's mobility in a city unobtrusively with taxis and detect flaws with implicit engagement of citizens.

## CONCLUSION

In this paper, we detect the flaws in the existing urban planning of a city using the GPS trajectories of taxis traveling in the urban areas. The detected results are comprised of two sets of findings. One is the frequent sub-graph patterns consisting of region pairs with salient traffic problems and the linking structure among these regions. The other is the association relations between these patterns. These results can first evaluate the effectiveness of the carried urban planning, and second provide a comprehensive view on the existing problem for decision-making when city planners conceive future plans. We executed our method based on real data generated by 30,000 taxis in Beijing in 2009 and 2010, and evaluated the

validity of our results using real urban planning of Beijing, including the newly built subway lines and roads and city projects that are still under construction. Some interesting discoveries are revealed from the data as well.

In the future, we might analyze how the detected flaws are derived from the existing urban planning by 1) studying the geographic features of a region, such as the road segments and points of interests, and 2) the purpose of people's travel, e.g., for shopping, sports, work etc.

## REFERENCES

1. Börzsönyi, S., Kossmann, D., Stocker, K. The skyline operator. In *Proc. ICDE 2001*. IEEE Press: 421-430.
2. Cranshaw, J., Toch, E., Hong, J. Kittur, A., Sadeh, N. Bridging the gap between the Physical Location and Online Social Networks. In *Proc. Ubicomp'10*, ACM Press (2010): 119-128.
3. Eagle, N., and Pentland, A. Reality mining: sensing complex social systems. *Personal Ubiquitous Computing*, 10, 4 (2006): 255-268.
4. Eagle, N., Montjoye, Y. D., and Bettencourt, L. Community Computing: Comparisons between Rural and Urban Societies using Mobile Phone Data, *IEEE Social Computing*, 144-150.
5. Ge, Y., Xiong, H., Tuzhilin, A., Xiao, K., Gruteser M., Pazzani M. J. An Energy-Efficient Mobile Recommender System. In *Proc. KDD 2010*, ACM Press (2010): 899-908.
6. Guehennemann A., Schaefer R. P., Thiessenhusen K. U., Wagner P. Monitoring traffic and emissions by floating car data. Institute of transport studies Australia; 2004.
7. Kindberg, T., Chalmers, M., Paulos, E. Gest editors' introduction: Urban computing. *Pervasive computing*. 6, 3 (2007), 18-20.
8. Kostakos V., O'Neill, E. Cityware: Urban computing to bridge online and real-world social networks. *Handbook of Research on Urban Informatics*, 2008.
9. Li, Q., Zheng, Y., Xie, X., Chen, Y., Liu, W., Ma, W.Y. Mining user similarity based on location history. In *Proc. GIS 2008*, ACM Press (2008): 1-10.
10. Liu, L., Andris, C., Biderman, A. and Ratti, C. Uncovering cabdrivers' behavior patterns from their digital traces. *Computers, Environment and Urban Systems*, 2010.
11. Rosenfeld, A. Connectivity in digital pictures. *Journal of the ACM (JACM)*, 17, 1(1970): 146-160.
12. Shklovski, I., Chang, M. F. Urban Computing-Navigating Space and Context. *IEEE Computer Society*. 39, 9 (2006), 36.
13. Yan, X., and Han, J. Discovery of frequent substructures. *Wiley-Interscience*, 2007. 99-113
14. Yuan J., Zheng Y., Xie, X., Sun, G. Driving with Knowledge from the Physical World. In *Proc. KDD 2011*, ACM Press 2011.
15. Yuan J., Zheng Y., Zhang C. Y., Xie, W., Xie, X., Sun, G. and Huang, Y. T-Drive: Driving Directions Based on Taxi Trajectories. In *Proc. GIS 2010*. ACM Press (2010), 99-108.
16. Ziebart, B., Maas, A., Dey, A. and Bagnell, J. Navigate like a cabbie: Probabilistic reasoning from observed context-aware behavior. In *Proc. Ubicomp 2008*, ACM Press (2008): 322.
17. Zheng, Y., Xie, X. and Ma, W. Y. GeoLife: A Collaborative Social Networking Service among User, Location and Trajectory. *IEEE Date Engineer Bulletin*, 33, 2 (2010), 32-40.
18. Zheng, Y., Zhang, L., Ma, Z., Xie, X., and Ma, W. Y. Recommending friends and locations based on individual location history. *ACM Trans. on the Web*, 5, 1 (2011), 1-44.